

Monitoring of changes in lipid profiles during PLK1 knockdown in cancer cells using DESI MS

Balasubramanyam Jayashree^{1,2} · Amitava Srimany³ · Srinidhi Jayaraman¹ · Anjali Bhutra¹ · Narayanan Janakiraman¹ · Srujana Chitipothu¹ · Subramanian Krishnakumar¹ · Lakshmi Subhadra Baddireddi² · Sailaja Elchuri¹ · Thalappil Pradeep³

Received: 12 April 2016 / Revised: 17 May 2016 / Accepted: 23 May 2016 / Published online: 8 June 2016
© Springer-Verlag Berlin Heidelberg 2016

Abstract The importance of the polo-like kinase 1 (PLK1) gene is increasing substantially both as a biomarker and as a target for highly specific cancer therapy. This is due to its involvement in multiple points of cell progression and carcinogenesis. PLK1 inhibitors' efficacy in treating human cancers has been limited due to the lack of a specific targeting strategy. Here, we describe a method of targeted downregulation of PLK1 in cancer cells and the concomitant rapid detection of surface lipidomic perturbations using desorption electrospray ionization mass spectrometry (DESI MS). The efficient delivery of siRNA targeting PLK1 gene selectively to the cancer cells is achieved by targeting overexpressed cell surface epithelial cell adhesion molecule (EpcAM) by the EpDT3 aptamer. The chimeric aptamer (EpDT3-siPLK1) showed the knockdown of PLK1 gene expression and PLK1 protein levels by quantitative PCR and western blotting, respectively. The abundant surface lipids, phosphatidylcholines

(PCs), such as PC(32:1) (*m/z* 754.6), PC(34:1) (*m/z* 782.6), and PC(36:2) (*m/z* 808.6), were highly expressed in MCF-7 and WERI-RB1 cancer cells compared to normal MIO-M1 cells and they were observed using DESI MS. These overexpressed cell surface lipids in the cancer cells were downregulated upon the treatment of EpDT3-siPLK1 chimera indicating a novel role of PLK1 to regulate surface lipid expression in addition to the efficient selective cancer targeting ability. Our results indicate that DESI MS has a potential ability to rapidly monitor aptamer-mediated cancer therapy and accelerate the drug discovery process.

Keywords Cancer · Aptamer · siPLK1 · DESI MS · Lipid

Introduction

Bilayer lipid membranes are essential parts of mammalian cells which consist of different phospholipids. These lipids are involved in different activities like cell signalling, metabolism, etc. Lipid composition of particular cell types changes due to different conditions of the cells. Several diseased conditions of cells, particularly tumors, can be understood by studying the lipid profiles of cells [1, 2]. Choline phospholipid metabolism is known to be dysregulated in cancers and has been used as diagnostic tools [3, 4]. The dysregulated choline metabolism as cancer biomarkers has been proposed using magnetic resonance spectroscopy [5, 6]. Mass spectrometry provides a simple way to capture molecule-specific lipid profiles of various tissues and cells. Incorporation of ambient ionization methods [7] makes the process of analysis faster and hassle free. Desorption electrospray ionization mass spectrometry (DESI MS) is one such ambient ionization process which was introduced in 2004 [8], and in fact, it is the first one of its kind.

Balasubramanyam Jayashree and Amitava Srimany contributed equally to this work.

Electronic supplementary material The online version of this article (doi:10.1007/s00216-016-9665-y) contains supplementary material, which is available to authorized users.

✉ Sailaja Elchuri
sailaja.elchuri@gmail.com

✉ Thalappil Pradeep
pradeep@iitm.ac.in

¹ Department of Nanobiotechnology, Vision Research Foundation, Sankara Nethralaya, Chennai, Tamil Nadu 600006, India

² Centre for Biotechnology, Anna University, Chennai, Tamil Nadu 600025, India

³ DST Unit of Nanoscience (DST UNS) and Thematic Unit of Excellence (TUE), Department of Chemistry, Indian Institute of Technology Madras, Chennai, Tamil Nadu 600036, India

DESI MS, being an ambient ionization technique, does not require extensive sample preparation and ionization occurs under atmospheric conditions, making the process highly compatible for biological sample analysis. It has been applied to several aspects of biological sciences. Examples include analysis of peptides [9], screening of different kinds of molecules from urine [10], study of animal tissue sections [11, 12], differentiation of tumor and non-tumor tissues [13, 14], identification of molecular species from plants [15], and spatial distribution of alkaloids in plant parts like seeds [16, 17], leaves and petals [18], etc. In spite of its diverse application in different areas of biology, the technique has not been used to study cell surface lipidomic changes upon targeted drug delivery.

Polo-like kinase 1 (PLK1) is a well-known oncogene that plays a major role in bipolar spindle formation [19, 20], chromosome segregation, centrosome maturation in late G2/early prophase [21], activation of Cdc25 [22], regulation of anaphase-promoting complex, and execution of cytokines [20, 23]. It is also involved in the direct phosphorylation of serine 62 of MYC protein and its stabilization [24] and regulates primary cilia disassembly in a kinase activity-dependent manner [25]. Thus, the importance of PLK1 is increasing substantially both as a biomarker and as a target for highly specific cancer therapy due to its involvement in multiple points of cell progression and carcinogenesis [26]. In addition to its role as mitotic check point, the role of PLK1 in signalling is well studied [27]. PLK1 signalling and lipid metabolism were the top dysregulated mechanisms in prostate cancer. The PLK1 signalling pathway and increased lipid expression led to prostate cancer progression [28]. However, PLK1-mediated lipid regulation, especially phosphatidylcholines which are considered as diagnostic markers for cancer, is lacking.

PLK1 inhibitors have already completed phase I clinical trials, but the efficacy of these agents in treating human cancers has been limited due to lack of specific targeting strategy. However, target-specific aptamer-siRNA conjugate against PLK1 could be a potential drug for cancer treatment. Aptamers are small single-stranded DNA/RNA molecules, described by a linear sequence of nucleotides, designed to specifically bind to a molecular target. They have low immunogenicity compared to proteins and therapeutic antibodies. Therefore, small DNA/RNA aptamers are identified for targeting cancer cells [29–33]. Aptamers have been designed against epithelial cell adhesion molecules (EpCAMs) which are highly expressed in most of the epithelial cancers [34]. Aptamer chimeras are generated using natural recombination or chemical processes. There is a possibility of losing the activity of one or both of the recombining partners during the process necessitating detailed investigations. An EpCAM aptamer-doxorubicin chimera was found to target the EpCAM positive cancer stem cells and deliver doxorubicin thereby leading to apoptosis of the cells [35]. The EpCAM aptamer

can be conjugated to a siRNA to target an oncogene such as PLK1 which is involved in G2/M cell cycle regulation to specifically target EpCAM positive cancers. Recently, EpCAM aptamer-PLK1 siRNA chimera has been found effective in mouse models of breast cancer [36]. Therefore, this chimera has been used presently to study PLK1-mediated lipid regulation in breast cancer and retinoblastoma cells.

In the present work, initially we established phosphatidylcholine signatures in cancer cell lines (MCF-7 and WERI-RB1) and compared it to a normal cell line (MIO-M1) to see if there are any cell-specific changes in the surface lipids between them using DESI MS. We then extended the study to see if the cancer-specific biomarker lipids could be regulated by giving targeted cancer drugs to understand therapy response. The aptamer drug EpDT3-siPLK1 targeted PLK1 gene leading to alterations in the surface lipidomic profiles. The use of DESI MS, in this context, provided a platform for rapid analysis of lipids from cells.

Materials and methods

Reagents

For cell culture, Roswell Park Memorial Institute 1640 (RPMI 1640), Dulbecco's Modified Eagle's Medium (DMEM), antibiotic-antimycotic solution, and fetal bovine serum (FBS) were purchased from Gibco Life Technologies, USA. For DESI MS experiments, HPLC grade methanol from Sigma-Aldrich, Germany and Whatman 42 filter paper from GE Healthcare UK Limited, UK were used.

Aptamer design

First, aptamer chimeras EpDT3-siPLK1 and EpDT3-siScr were designed. The lengths of the chimeras were designed to be 60 nucleotides containing a Dicer recognition site between the EpCAM aptamer and the PLK1 siRNA sequence. To increase the stability of the aptamer chimeras against endogenous nucleases, modification was made by adding 2-nucleotide 3' overhangs. The aptamer was fluorescently labelled at the 3' end to visualize binding of chimeras to the cells. All the RNA sequences including the aptamer chimera sequences were designed and HPLC purified by Dharmacon, USA.

Cell culture

Retinoblastoma WERI-RB1 cells (obtained from RIKEN BioResource Center, Ibaraki, Japan) were maintained in RPMI 1640, with 10 % FBS, and supplemented with antibiotic-antimycotic solution containing penicillin 100 µg/ml, streptomycin 100 µg/ml, and amphotericin B

250 ng/ml. Breast cancer cell line Michigan Cancer Foundation-7 (MCF-7) was procured from the American Type Culture Collection (ATCC), Manassas, VA, USA, and Müller Glial MIO-M1 cell line was a kind gift from Professor Astrid Limb, London, UK, and they were cultured in DMEM containing 10 % FBS with and without antibiotic-antimycotic solution, respectively. All the cell lines were maintained in a 5 % CO₂ environment at 37 °C.

Flow cytometry

Cells (4×10^5 ; MIO-M1, MCF-7 or WERI-RB1) were collected and washed twice with cold phosphate-buffered saline (PBS). Cells were then resuspended in blocking buffer (PBS with 0.02 % sodium azide, 0.1 % FBS, and 0.01 % Triton X-100) and incubated with different concentrations (100–500 nM) of fluorescein isothiocyanate (FITC)-tagged aptamer chimeras (EpDT3-siPLK1 and EpDT3-siScr). After 1 h, the cells were washed twice with cold PBS and resuspended in sheath fluid. Cells (10^4) were collected and analyzed using FACS.

Dicer cleavage assay

EpDT3-siPLK1 chimera (100 nM) was denatured by heating for 10 min in a boiling water bath. Digestion using Dicer enzyme was set up as per the manufacturer's protocol (Recombinant Dicer Kit) with and without Dicer. The samples were then resolved using native PAGE (15 % w/v polyacrylamide) and stained with ethidium bromide before visualization using the Gel Doc (Bio-Rad).

Quantitative RT-PCR

MIO-M1, MCF-7, and WERI-RB1 cells were transfected with 100 nM of EpDT3, Scr-EpDT3, 150 nM of siPLK1, siScr, EpDT3-siPLK1, and EpDT3-siScr. The cells were harvested after 48 h and washed twice with cold PBS. RNA was extracted with TRIzol reagent using an optimized protocol and reverse transcribed into cDNA using High-Capacity cDNA Reverse Transcription Kit (Applied Biosystems). Quantitative RT-PCR was performed with SYBR Green (Applied Biosystems) using GAPDH as endogenous control. The primers used were FP 5'-GACAAGTACGGCCTTGGGTA and RP 5'-GTGCCGTCACGCTCTATGTA for PLK1 (Sigma-Aldrich) and FP 5'-AGAAGGCTGGGGCTCATTTG and RP 5'-AGGGGCCATCCACAGTCTTC for GAPDH (Sigma-Aldrich). The threshold cycle (Ct) values obtained from Applied Biosystems were used to calculate relative quantification with the formula $2^{-\Delta\Delta C_t}$, where $\Delta\Delta C_t$ are the values obtained on normalizing the values of

treated samples with values of untreated and endogenous controls.

Western blotting

MIO-M1, MCF-7, and WERI-RB1 cells were transfected with 150 nM of EpDT3, siPLK1, siScr, EpDT3-siPLK1, and EpDT3-siScr and they were collected after 48 h. The cells were then lysed in RIPA buffer containing Protease Inhibitor Cocktail (Sigma-Aldrich) followed by cold PBS wash. Supernatant was collected after centrifuging the samples for 10 min at 10,000 rpm. The lysates obtained were estimated using Bradford method against BSA standard. Protein (75 μ g) was resolved on a 10 % SDS-PAGE and transferred onto a nitrocellulose membrane. The blot was blocked for 1 h with 5 % skimmed milk and the membrane was probed with anti-PLK1 primary monoclonal antibody (Invitrogen: 37–7000) at 1:1000 dilution. The primary antibody was treated overnight at 4 °C. Then, the blot was washed three times with PBST and probed with secondary anti-mouse conjugated with HRP (Santa Cruz Biotechnology: sc-2005) at 1:4500 dilution for 1 h. The membrane was detected using a TMB substrate (Merck). GAPDH (Sigma-Aldrich: G8795) was used as endogenous control. ImageJ software was used to normalize treated samples with control samples and represented in ratio with GAPDH.

Statistical analysis

For quantitative RT-PCR and western blotting experiments, data were obtained in triplicates and the comparisons were performed using Student's *t*-test. *P* values less than 0.05 were considered as statistically significant.

DESI MS

After treatment with 150 nM siPLK1 and EpDT3-siPLK1 for 48 h, cells were collected and washed in cold PBS. The pellet was resuspended in 10 μ l PBS. Then, 5 μ l of cell suspension was spotted on Whatman 42 filter paper and it was kept in normal lab conditions for about 5 min to dry. Then, the paper containing the cells was fixed on the glass slide used in the DESI MS stage. Our previous study demonstrated that spotting cells on Whatman 42 filter paper could identify surface lipids more efficiently compared to other common surfaces used in DESI MS analysis [37]. Here we have used the same methodology. A 2D DESI MS source from Prosolia, Inc. was used for all mass spectrometric measurements. The source was connected with a Thermo LTQ XL ion trap mass spectrometer. DESI MS data were acquired in positive ion mode with 5 kV spray voltage. HPLC grade methanol was used as solvent and it was sprayed at 5 μ l/min flow rate with the help of 150 psi nebulizer gas pressure. The data obtained was

processed by FireFly software to make images and the images were viewed by BioMap software. Collision-induced dissociation (CID) was used for tandem mass spectrometry (MS/MS) experiments.

Gene microarray analysis

To understand the global gene expression changes accompanying the PLK1 knockdown leading to dysregulated lipidomic signature and cancer cell death, whole genome microarray experiments were undertaken. The control MCF-7 and EpDT3-siPLK1-treated MCF-7 cells were evaluated for gene expression using Affymetrix GeneChip PrimeView Human Gene Expression Array according to the manufacturer's protocol. Briefly, the samples were collected after treatment and ribonucleic acid was extracted from each of the samples using RNeasy kit (QIAGEN, Valencia, CA) and hybridized to GeneChip PrimeView Human Gene Expression Array (Affymetrix, Santa Clara, CA). Microarray data from the samples were background corrected and normalized using the GCRMA algorithm. One probe set per gene, based on highest overall expression level across samples, was selected for use in subsequent analyses. Differential expression of genes was determined using Student's *t*-test. Gene expression array data were generated and analyzed as described. The Gene Ontology (GO) was performed using GeneSpring 13.0 (Agilent Technologies). The top GO processes are presented at <0.05 significance levels.

MTT assay

Following 48 h transfection, cells were incubated with MTT (5 mg/ml) for 4 h at 37 °C. After 4 h, the formazan crystals were formed and on addition of DMSO the purple color of formazan was observed. The absorbance was measured at 570 nm on ELISA plate reader.

Results and discussion

Targeted aptamer-mediated PLK1 gene regulation

For targeted cancer therapy, an aptamer (EpDT3) which selectively targets EpCAM expressed cancer cells was chosen and conjugated with PLK1 targeting siRNA to construct EpDT3-siPLK1 chimera. This was used to knockdown the expression of PLK1, specifically in cancer cells (expressing EpCAM) and not in the normal cells. A Dicer cleavage site was incorporated in the aptamer chimera for the enzyme Dicer to recognize and guide the siRNA into the RNAi pathway enabling the efficient downregulation of the PLK1 gene. The secondary structure prediction of the EpDT3-siPLK1 chimera (see Electronic Supplementary Material (ESM) Fig. S1) was done using

RNAstructure, version 5.0. A scrambled siRNA sequence linked to EpCAM aptamer (EpDT3-siScr, ESM Fig. S1) was used as control. The silencing activity and specificity of aptamer-siRNA chimeras are generally increased by incorporating modifications that enable more efficient processing of the siRNA by the cellular machinery. These include adding of 2-nucleotide 3' overhangs, optimizing the thermodynamic profile, and structuring of the duplex to favor the processing of siRNA guide strand. These modifications had been previously employed to enable the PSMA aptamer chimeras to specifically target prostate cancer cells compared to normal cells [38]. Unlike the PSMA that targets only prostate cancer cells, the present aptamer chimera has potential to target all cancer cells that overexpress cell surface molecule EpCAM which include breast, pancreas, lung, colon, and liver enabling the wider application of the drug for targeted cancer therapy. The MCF-7 cell line with 98 % EpCAM expression [39] was chosen for the aptamer chimera drug treatment. A retinoblastoma cell line WERI-RB1 with 41 % EpCAM expression [35] was chosen to study the drug uptake in mixed (high and low) EpCAM-expressing cell populations. A normal cell line MIO-M1 with low EpCAM expression was taken as control.

We first performed binding studies of the chimeras on cancer cells and normal cells to assess its specificity to the cancer cells. Flow cytometry was used for this purpose. Previous studies showed that the percentage of aptamer binding to the cells can be evaluated by flow cytometry using FITC as fluorescent label [40]. Thus, to track the binding efficiency of EpDT3-siPLK1 and EpDT3-siScr, FITC labelling was done and its cellular uptake was evaluated. Increasing concentrations of the EpDT3-siPLK1 chimera (100 to 500 nM) were used to assess its binding efficiency to the cells. MIO-M1, a non-cancerous cell which expresses low levels of EpCAM, when incubated with 100 nM of EpDT3-siPLK1, showed a very minimal binding of 4–6.6 % (ESM Fig. S2A) which was found to be nearly the same when chimera concentration was increased to 500 nM, correlating to the fact that MIO-M1 has low EpCAM expression. For MCF-7, having 98 % EpCAM expression [39], the binding efficiency was found to increase from 90 to 96 % when chimera concentration was increased from 100 to 300 nM and then saturated (ESM Fig. S2B). In case of WERI-RB1, having 41 % EpCAM expression, a binding efficiency of nearly 27 % was observed with 500 nM chimera concentration (ESM Fig. S2C). A bimodal distribution (ESM Fig. S2C) indicates a subset of cellular populations having higher aptamer uptake while another subset having lower aptamer uptake. The percentage binding of EpDT3-siPLK1 is in agreement with EpCAM protein expression reported previously in WERI-RB1 cell line using EpCAM antibody [35]. The EpDT3-siScr chimera exhibited 5, 96, and 26 % binding in MIO-M1, MCF-7, and WERI-RB1, respectively (ESM Fig. S3). Both the EpDT3-siPLK1 and EpDT3-siScr chimeras showed almost similar binding efficiencies.

For EpDT3-siPLK1 chimera to enter into the RNAi pathway, it is important that siPLK1 is released from the chimera and this aspect was tested by an *in vitro* cleavage assay. General reports say that a pre-microRNA can be cleaved by an enzyme Droscha, processed by Dicer endonuclease, into a 21-nt mature miRNA which enters RNA-induced silencing complex (RISC) for the mRNA degradation leading to the downregulation of the gene expression process. When EpDT3-siPLK1 was incubated with recombinant Dicer, it was digested to an expected 20–22-nt cleavage product. Two distinct bands were seen in gel electrophoresis: lower band representing EpDT3 and upper band due to siPLK1 (ESM Fig. S4). The data suggested that Dicer enzyme could cleave the EpDT3-siPLK1 chimera *in vitro* into EpDT3 and siPLK1. We suggest a similar release of siPLK1 inside the cells and thereby leading to the regulation of PLK1 expression.

Targeted silencing of a particular gene by using an aptamer has already been implied in cancer research and has been found to be very specific for reducing tumor growth [38, 41]. Therefore, the efficacy of PLK1 regulation by the aptamer was studied. The gene expression was studied in MIO-M1, MCF-7, and WERI-RB1 cells by quantitative RT-PCR (Fig. 1A–C). The levels of PLK1 remained unchanged when treated with only EpDT3, Scr-EpDT3, and siScr in all three cell lines indicating that EpDT3 aptamer alone and scrambled siRNA sequence had no effect on the PLK1 gene expression. In normal MIO-M1 cells, the level of PLK1 was reduced when treated with siPLK1 and had no effect on treatment with EpDT3-siPLK1 chimera (Fig. 1A) indicating that the aptamer chimera could not bind to MIO-M1 cells due to low expression of EpCAM. This indicates non-target ability of the EpDT3-siPLK1 chimera to normal cells with reduced EpCAM expression. The use of siPLK1 alone resulted in regulation of PLK1 in non-cancerous cells too. The PLK1 gene

expression was reduced both by siPLK1 and EpDT3-siPLK1 in both the cancer cell lines (MCF-7 and WERI-RB1) after 48 h of treatment (Fig. 1B, C). The data suggest that EpDT3-siPLK1 could regulate PLK1 gene expression in cells overexpressing EpCAM. The target-specific delivery method is more efficient than Lipofectamine-delivered siRNA, as Lipofectamine delivers siRNA non-specifically into all the cells by electrostatic interactions, whereas our chimera delivers the siRNA by cell type-specific molecular recognition. In case of EpDT3-siScr, though the surface binding through EpCAM was almost the same as EpDT3-siPLK1 (ESM, Figs. S2 and S3), the knockdown of PLK1 was not seen (Fig. 1B, C) because the scrambled siRNA could not regulate PLK1 gene expression indicating the specificity of EpDT3-siPLK1 for PLK1 gene regulation. In agreement with mRNA levels, the PLK1 protein levels were also reduced in MCF-7 (Fig. 1D) and WERI-RB1 (Fig. 1E) cells after 48 h of EpDT3-siPLK1 treatments. Since EpDT3-siPLK1 binding was minimal in WERI-RB1 (27 %), the knockdown created by EpDT3-siPLK1 was lower compared to normal siRNA transfection (Fig. 1E). EpDT3-siScr had no effect on the PLK1 protein expression. Thus, EpDT3-siPLK1 selectively targets PLK1 in cancer cells sparing the normal cells.

Surface lipidomic signatures of cancer cells can be altered using EpDT3-siPLK1

DESI MS experiments were performed to understand the lipid profiles of different cells. Positive mode DESI MS spectra of MIO-M1, MCF-7, and WERI-RB1 cell lines are shown in Fig. 2. All the mass spectra were recorded between m/z 700 and 900 as this region exhibited intense lipid peaks. The lipids were identified by tandem DESI MS experiments and using database (www.lipidmaps.org) as reference. MS/MS data of

Fig. 1 Expression of PLK1 gene in (A) MIO-M1, (B) MCF-7, and (C) WERI-RB1 when they were untreated (1) and treated with EpDT3 (2), Scr-EpDT3 (3), siPLK1 (4), siScr (5), EpDT3-siPLK1 (6), and EpDT3-siScr (7). Expression of PLK1 protein in (D) MCF-7 and (E) WERI-RB1 when they were untreated (1) and treated with EpDT3 (2), siPLK1 (3), siScr (4), EpDT3-siPLK1 (5), and EpDT3-siScr (6). * $P < 0.05$ compared to untreated

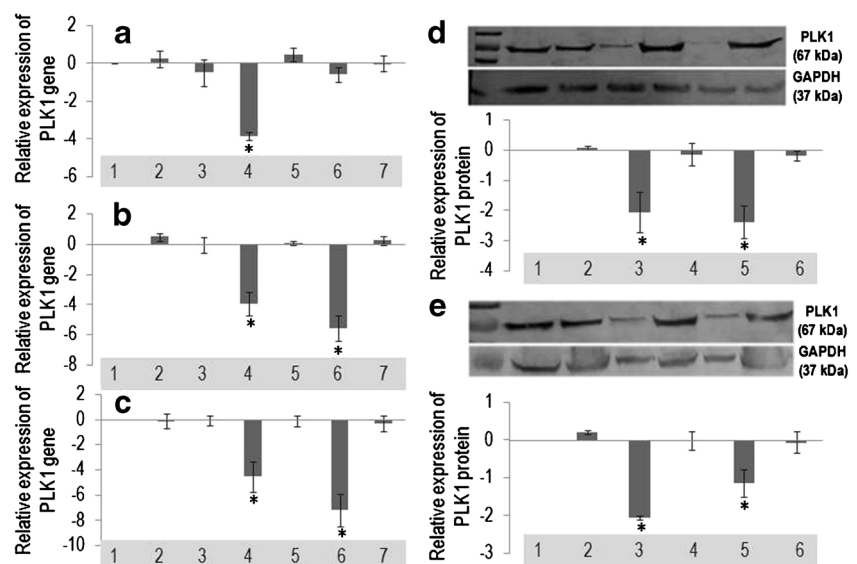
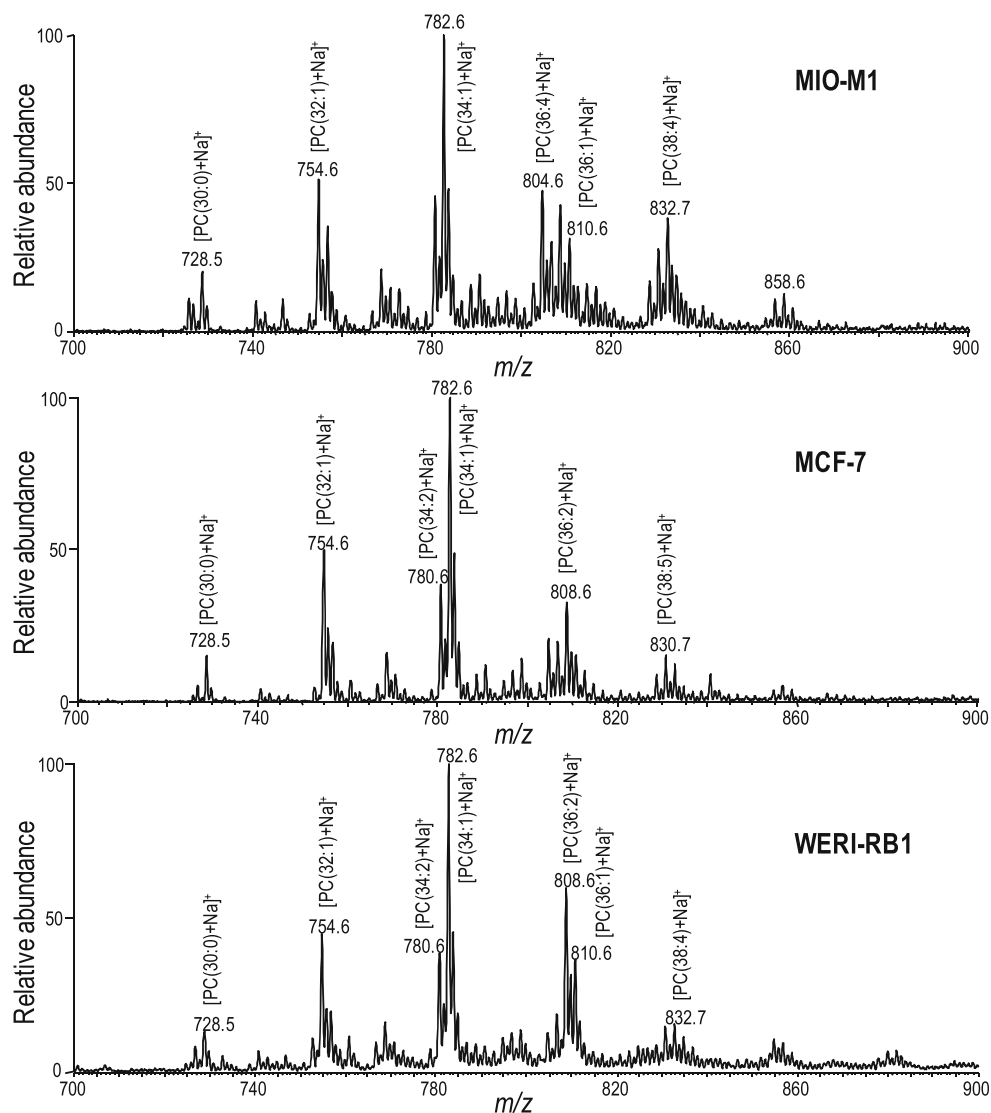


Fig. 2 Positive mode DESI MS spectra of MIO-M1, MCF-7, and WERI-RB1 cell lines from Whatman 42 filter paper



three major peaks (m/z 754.6, m/z 782.6, and m/z 808.6) from MCF-7 cell line are shown in ESM Fig. S5. All the three spectra show characteristic losses of 59 and 183 Da indicating the species as phosphatidylcholines. The highly abundant lipids (m/z 754.6, m/z 782.6, and m/z 808.6) from both the cancer cell lines (MCF-7 and WERI-RB1) were chosen and their intensities were compared with a normal cell line, MIO-M1. Figure 3 shows the comparison of the ion intensities of the lipids between MIO-M1/MCF-7 and MIO-M1/WERI-RB1 pairs. In both the cases, these lipids were highly expressed in tumor cells than the normal cells. When compared to MIO-M1, the relative expressions of the lipids were much higher in WERI-RB1 than in MCF-7. Figures S6 and S7 in the ESM show comparisons of several other lipids between MIO-M1/MCF-7 and MIO-M1/WERI-RB1 pairs, respectively. However, all these minor peaks did not show upregulation in cancer cells compared to normal cell. A few minor peaks were upregulated in MIO-M1 cells compared to cancer cells

(ESM, Figs. S6 and S7). It is noteworthy to mention at this point that a simple spot sampling could have been done to get similar information instead of DESI MS imaging experiments. However, we have chosen DESI MS imaging over spot sampling due to the fact that in an imaging experiment, sampling is more uniform than a spot sampling experiment. Moreover, images provide better visualization of data for comparison and that too considering the whole sample. Furthermore, as we had not used any internal standards in our experiments and DESI MS is a semi-quantitative technique, comparisons between samples were made from images on a semi-quantitative basis. Besides, use of such standards has inherent problem in this situation as sampled lipids are part of the cell structure while reference samples added are loosely bound and are therefore easier to desorb from surface.

In MYC-induced mouse lymphoma samples, it was shown earlier by DESI MS that some lipids had increased abundances while some had decreased abundances [42]. In another

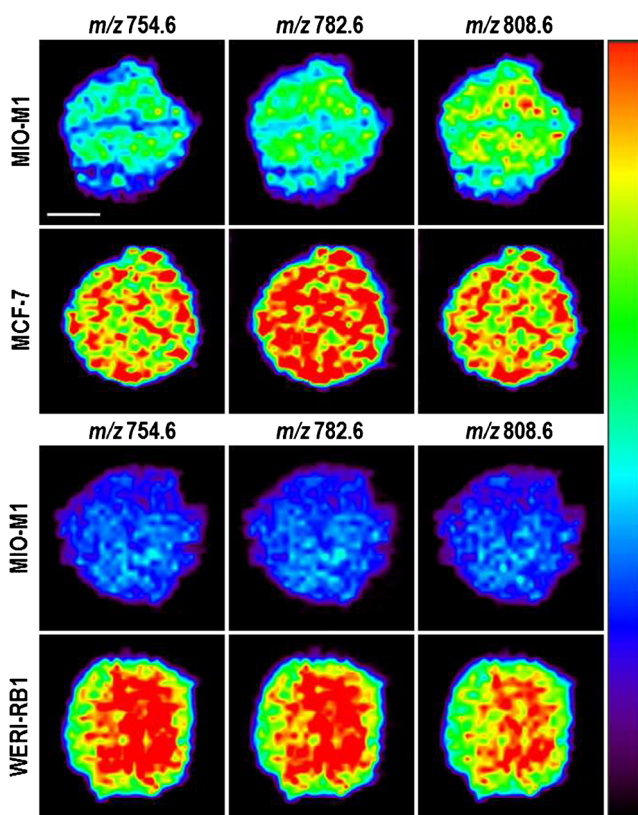


Fig. 3 DESI MS images of different lipids from MIO-M1/MCF-7 and MIO-M1/WERI-RB1 cell lines. *Scale bar* of 2 mm applies to all the images. Intensity is color coded, from *black* (low) to *red* (high)

study, using 2D liquid chromatography-mass spectrometry method, two phosphatidylinositol (PI) lipids, PI(16:0/16:1) and PI(18:0/20:4), were identified as potential biomarkers to differentiate benign and malignant breast tumors [43]. Phosphatidylcholines had been proposed as possible biomarkers using ultra performance liquid chromatography electrospray ionization time-of-flight mass spectrometry (UPLC-ESI-TOF-MS) in esophageal squamous cell carcinoma [44]. Here, in our study, the cancer cell-specific phosphatidylcholine lipids have been identified using the rapid method of DESI MS with minimum sample preparation. The change in the abundances of phosphatidylcholines on the cancer cell surface compared to normal cell surface could be due to altered lipid synthesis/degradation mechanism.

Effect of targeted delivery of EpDT3-siPLK1 was manifested in the surface lipid profiles of cancer cell lines and it was monitored by DESI MS. Figures 4 and 5 show the DESI MS images of MCF-7 and WERI-RB1 cells, respectively, in different treatment conditions. It was found that the major peaks at m/z 754.6, m/z 782.6, and m/z 808.6 that showed upregulation in both the cancer cell lines compared to the normal cell line were downregulated when treated with both siPLK1 and EpDT3-siPLK1. In MCF-7 cells, the differences in the intensity reduction between Lipofectamine-transfected siRNA and

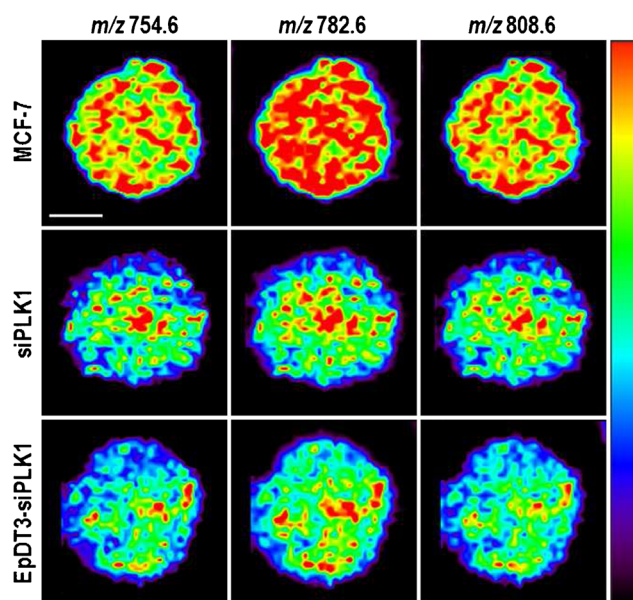


Fig. 4 DESI MS images of different lipids from MCF-7 cells with different treatment conditions. *Scale bar* of 2 mm applies to all the images. Intensity is color coded, from *black* (low) to *red* (high)

aptamer-mediated siRNA were almost the same (Fig. 4). Since most of the MCF-7 cells express EpCAM, equal reduction explains the fact that the siRNA delivered by EpDT3-siPLK1 was almost similar to that delivered by Lipofectamine. However, in the WERI-RB1 cells, the magnitudes of the decrease in the intensities of the lipids were not the same for siPLK1 and EpDT3-siPLK1-treated cells (Fig. 5). The untargeted siPLK1 caused reduction in entire cellular population resulting in much lowered cell

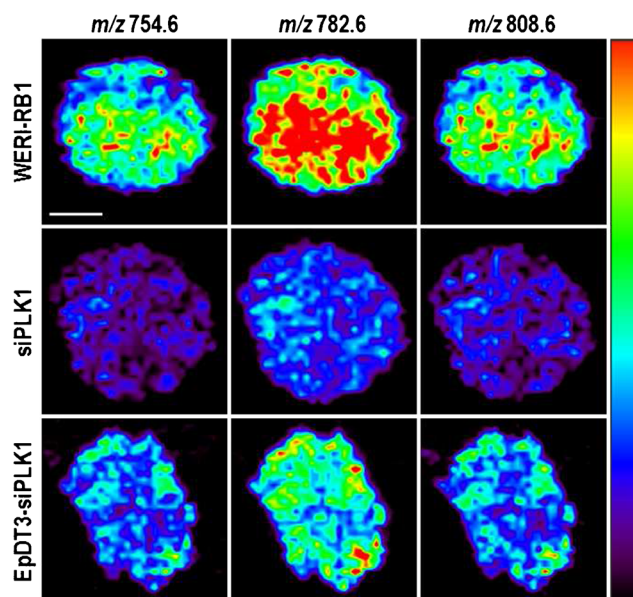


Fig. 5 DESI MS images of different lipids from WERI-RB1 cells with different treatment conditions. *Scale bar* of 2 mm applies to all the images. Intensity is color coded, from *black* (low) to *red* (high)

surface lipids. In WERI-RB1, the EpCAM is expressed in 41 % cells. Therefore, when treated with EpDT3-siPLK1, the intensity reduction of the lipids was minimal when compared to siPLK1 treatment alone. Figures S8 and S9 in the ESM show DESI MS images of few other lipids from MCF-7 and WERI-RB1 cell lines, respectively, when they were treated with siPLK1 and EpDT3-siPLK1. The same trend of major peaks was also observed for minor peaks, although all these minor peaks did not show upregulation in cancer cells compared to normal cells (ESM, Figs. S6 and S7).

The reduction in PLK1 gene expression reduced the lipid expression, phosphatidylcholines in particular, suggesting a novel functional role of PLK1 in lipid synthesis/degradation in addition to its role in mitotic spindle formation, cellular proliferation, cell migration, and cell death. To identify the genes regulated by PLK1, whole genome microarray analysis was done in MCF-7 cells (ESM Fig. S10). We found changes in 2380 genes compared to the control. However, 254 genes showed fold change differences of 2. 143 genes were downregulated and 111 genes were upregulated (ESM Table S1). We did not find variation in genes related to phosphatidylcholine synthesis. However, upregulation of PLA2G4C which are involved in phosphatidylcholine degradation accounts for decreased phosphatidylcholines after the treatment of EpDT3-siPLK1. Previously, an altered choline metabolism with increased expression of choline synthesizing pathway enzymes such as choline kinase and decreased expression of lipid degradation pathway enzymes including phospholipase A2 was observed in breast cancer cell line compared to normal cell line [4]. In our study, aptamer therapy is manifested by decreased phosphatidylcholines and observed by rapid method of DESI MS indicating suitability of DESI MS for rapid drug screening and therapy response.

Increased cell death is indicative of therapy by EpDT3-siPLK1

To confirm the cytotoxic effect due to the targeted delivery by EpDT3-siPLK1 on cancer cells, MTT assay was performed. The results showed that the aptamer drug treatment increased cell death in both MCF-7 and WERI-RB1 cells (ESM Fig. S11), indicating the potential application of this aptamer chimera for targeted drug delivery. The global gene expression regulated by aptamer chimera treatment was performed to understand the changes accompanying cancer cell death in MCF-7 cells. A reduction in oncogenes such as PLK1 and NRAS has been observed (ESM Table S1). The Gene Ontology analysis by GeneSpring software for the genes dysregulated by 2 folds has revealed processes associated with

macromolecule metabolism, cellular metabolism, cell death, apoptosis, centromere complex assembly, DNA conformation change, chromatin assembly, and phosphatidylinositol-mediated signalling altered by depleted PLK1 (ESM Table S2). PLK1 downregulation has increased processes related to apoptosis and cell death accounting for observed increased cell death by EpDT3-siPLK1. The degradation products of lipids such as phosphatidylinositol and ceramide (signalling lipids) are known to play a role in cellular apoptosis and proliferation pathways [45]. The mechanism of lipid degradation by the aptamer chimera treatment to trigger apoptosis is currently under investigation.

Conclusions

In summary, an EpCAM aptamer chimera, EpDT3-siPLK1, was used for targeted drug delivery in MCF-7 and WERI-RB1 cells. It bounds more efficiently with highly EpCAM-expressing MCF-7 cells than WERI-RB1 cells where EpCAM expression is less. PLK1 gene expression and corresponding protein levels were reduced by the action of the chimera. DESI MS showed that surface lipids of the cells were also affected by aptamer chimera treatment suggesting novel role of PLK1 in regulating lipids in the cells. This approach of surface lipid profiling of treated cells described herein can be a prospective new method to identify new biomarkers for rapid drug screening.

Acknowledgments This work was supported by the Department of Biotechnology, Government of India (Grant no. NO.BT/PR3580/PID/6/625/2011) and the Department of Science and Technology, Government of India. A.S. thanks the Council of Scientific and Industrial Research, Government of India and Indian Institute of Technology Madras for fellowships. The authors also thank Dr. Nithya Subramanian, Ms. Srilatha Jasty, and Ms. Lakshmi for their help and suggestions.

Compliance with ethical standards

Conflict of interest The authors declare that they have no conflict of interest.

References

1. Beljebbar A, Dukic S, Amharref N, Bellefqih S, Manfait M. Monitoring of biochemical changes through the C6 gliomas progression and invasion by Fourier transform infrared (FTIR) imaging. *Anal Chem.* 2009;81:9247–56.
2. Shimma S, Sugiura Y, Hayasaka T, Hoshikawa Y, Noda T, Setou M. MALDI-based imaging mass spectrometry revealed abnormal distribution of phospholipids in colon cancer liver metastasis. *J Chromatogr B.* 2007;855:98–103.

3. Ackerstaff E, Glunde K, Bhujwala ZM. Choline phospholipid metabolism: a target in cancer cells? *J Cell Biochem.* 2003;90:525–33.
4. Glunde K, Jie C, Bhujwala ZM. Molecular causes of the aberrant choline phospholipid metabolism in breast cancer. *Cancer Res.* 2004;64:4270–6.
5. Gillies RJ, Morse DL. In vivo magnetic resonance spectroscopy in cancer. *Annu Rev Biomed Eng.* 2005;7:287–326.
6. Glunde K, Artemov D, Penet M-F, Jacobs MA, Bhujwala ZM. Magnetic resonance spectroscopy in metabolic and molecular imaging and diagnosis of cancer. *Chem Rev.* 2010;110:3043–59.
7. Monge ME, Harris GA, Dwivedi P, Fernandez FM. Mass spectrometry: recent advances in direct open air surface sampling/ionization. *Chem Rev.* 2013;113:2269–308.
8. Takats Z, Wiseman JM, Gologan B, Cooks RG. Mass spectrometry sampling under ambient conditions with desorption electrospray ionization. *Science.* 2004;306:471–3.
9. Pasilis SP, Kertesz V, Van Berkel GJ, Schulz M, Schorch S. HPTLC/DESI-MS imaging of tryptic protein digests separated in two dimensions. *J Mass Spectrom.* 2008;43:1627–35.
10. Chipuk JE, Gelb MH, Brodbelt JS. Rapid and selective screening for sulfhydryl analytes in plasma and urine using surface-enhanced transmission mode desorption electrospray ionization mass spectrometry. *Anal Chem.* 2010;82:4130–9.
11. Wiseman JM, Ifa DR, Venter A, Cooks RG. Ambient molecular imaging by desorption electrospray ionization mass spectrometry. *Nat Protoc.* 2008;3:517–24.
12. Vismeh R, Waldon DJ, Teffera Y, Zhao Z. Localization and quantification of drugs in animal tissues by use of desorption electrospray ionization mass spectrometry imaging. *Anal Chem.* 2012;84:5439–45.
13. Eberlin LS, Norton I, Orringer D, Dunn IF, Liu X, Ide JL, et al. Ambient mass spectrometry for the intraoperative molecular diagnosis of human brain tumors. *Proc Natl Acad Sci U S A.* 2013;110:1611–6.
14. Eberlin LS, Tibshirani RJ, Zhang J, Longacre TA, Berry GJ, Bingham DB, et al. Molecular assessment of surgical-resection margins of gastric cancer by mass-spectrometric imaging. *Proc Natl Acad Sci U S A.* 2014;111:2436–41.
15. Srimany A, Ifa DR, Naik HR, Bhat V, Cooks RG, Pradeep T. Direct analysis of camptothecin from *Nothapodytes nimmoniana* by desorption electrospray ionization mass spectrometry (DESI-MS). *Analyst.* 2011;136:3066–8.
16. Ifa DR, Srimany A, Eberlin LS, Naik HR, Bhat V, Cooks RG, et al. Tissue imprint imaging by desorption electrospray ionization mass spectrometry. *Anal Methods.* 2011;3:1910–2.
17. Mohana Kumara P, Srimany A, Ravikanth G, Uma Shaanker R, Pradeep T. Ambient ionization mass spectrometry imaging of rohitukine, a chromone anti-cancer alkaloid, during seed development in *Dysoxylum binectariferum* Hook.f (Meliaceae). *Phytochemistry.* 2015;116:104–10.
18. Hemalatha RG, Pradeep T. Understanding the molecular signatures in leaves and flowers by desorption electrospray ionization mass spectrometry (DESI MS) imaging. *J Agric Food Chem.* 2013;61:7477–87.
19. Glover DM, Hagan IM, Tavares ÁAM. Polo-like kinases: a team that plays throughout mitosis. *Gene Dev.* 1998;12:3777–87.
20. Glover DM, Ohkura H, Tavares A. Polo kinase: the choreographer of the mitotic stage? *J Cell Biol.* 1996;135:1681–4.
21. Nigg EA, Blangy A, Lane HA. Dynamic changes in nuclear architecture during mitosis: on the role of protein phosphorylation in spindle assembly and chromosome segregation. *Exp Cell Res.* 1996;229:174–80.
22. Kumagai A, Dunphy WG. Purification and molecular cloning of Plx1, a Cdc25-regulatory kinase from *Xenopus* egg extracts. *Science.* 1996;273:1377–80.
23. Nigg EA. Polo-like kinases: positive regulators of cell division from start to finish. *Curr Opin Cell Biol.* 1998;10:776–83.
24. Cunningham JT, Ruggero D. New connections between old pathways: PDK1 signaling promotes cellular transformation through PLK1-dependent MYC stabilization. *Cancer Discov.* 2013;3:1099–102.
25. Wang G, Chen Q, Zhang X, Zhang B, Zhuo X, Liu J, et al. PCM1 recruits Plk1 to the pericentriolar matrix to promote primary cilia disassembly before mitotic entry. *J Cell Sci.* 2013;126:1355–65.
26. Cholewa BD, Liu X, Ahmad N. The role of polo-like kinase 1 in carcinogenesis: cause or consequence? *Cancer Res.* 2013;73:6848–55.
27. Bholra NE, Jansen VM, Bafna S, Giltman JM, Balko JM, Estrada MV, et al. Kinome-wide functional screen identifies role of PLK1 in hormone-independent, ER-positive breast cancer. *Cancer Res.* 2015;75:405–14.
28. Zhang Z, Hou X, Shao C, Li J, Cheng J-X, Kuang S, et al. Plk1 inhibition enhances the efficacy of androgen signaling blockade in castration-resistant prostate cancer. *Cancer Res.* 2014;74:6635–47.
29. Denholt CL, Hansen PR, Pedersen N, Poulsen HS, Gillings N, Kjær A. Identification of novel peptide ligands for the cancer-specific receptor mutation EFGFRvIII using a mixture-based synthetic combinatorial library. *Biopolymers.* 2009;91:201–6.
30. Kim M, Shin D-S, Kim J, Lee Y-S. Substrate screening of protein kinases: detection methods and combinatorial peptide libraries. *Biopolymers.* 2010;94:753–62.
31. Li J, Tan S, Chen X, Zhang CY, Zhang Y. Peptide aptamers with biological and therapeutic applications. *Curr Med Chem.* 2011;18:4215–22.
32. Pirogova E, Istivan T, Gan E, Cosic I. Advances in methods for therapeutic peptide discovery, design and development. *Curr Pharm Biotechnol.* 2011;12:1117–27.
33. Aina OH, Liu R, Sutcliffe JL, Marik J, Pan C-X, Lam KS. From combinatorial chemistry to cancer-targeting peptides. *Mol Pharmaceutics.* 2007;4:631–51.
34. Zhu Z, Song Y, Li C, Zou Y, Zhu L, An Y, et al. Monoclonal surface display SELEX for simple, rapid, efficient, and cost-effective aptamer enrichment and identification. *Anal Chem.* 2014;86:5881–8.
35. Subramanian N, Raghunathan V, Kanwar JR, Kanwar RK, Elchuri SV, Khetan V, et al. Target-specific delivery of doxorubicin to retinoblastoma using epithelial cell adhesion molecule aptamer. *Mol Vis.* 2012;18:2783–95.
36. Gilboa-Geffen A, Hamar P, Le MTN, Wheeler LA, Trifonova R, Petrocca F, et al. Gene knockdown by EpCAM aptamer-siRNA chimeras suppresses epithelial breast cancers and their tumor-initiating cells. *Mol Cancer Ther.* 2015;14:2279–91.
37. Srimany A, Jayashree B, Krishnakumar S, Elchuri S, Pradeep T. Identification of effective substrates for the direct analysis of lipids from cell lines using desorption electrospray ionization mass spectrometry. *Rapid Commun Mass Spectrom.* 2015;29:349–56.
38. Dassie JP, Liu XY, Thomas GS, Whitaker RM, Thiel KW, Stockdale KR, et al. Systemic administration of optimized aptamer-siRNA chimeras promotes regression of PSMA-expressing tumors. *Nat Biotechnol.* 2009;27:839–49.
39. Subramanian N, Kanwar JR, Athalya PK, Janakiraman N, Khetan V, Kanwar RK, et al. EpCAM aptamer mediated cancer cell specific delivery of EpCAM siRNA using polymeric nanocomplex. *J Biomed Sci.* 2015;22:4.
40. Liu HY, Gao X. A universal protein tag for delivery of siRNA-aptamer chimeras. *Sci Rep.* 2013;3:3129.
41. Zhou J, Tiemann K, Chomchan P, Alluin J, Swiderski P, Burnett J, et al. Dual functional BAFF receptor aptamers inhibit ligand-induced proliferation and deliver siRNAs to NHL cells. *Nucleic Acids Res.* 2013;41:4266–83.

42. Eberlin LS, Gabay M, Fan AC, Gouw AM, Tibshirani RJ, Felsher DW, et al. Alteration of the lipid profile in lymphomas induced by MYC overexpression. *Proc Natl Acad Sci U S A*. 2014;111:10450–5.
43. Yang L, Cui X, Zhang N, Li M, Bai Y, Han X, et al. Comprehensive lipid profiling of plasma in patients with benign breast tumor and breast cancer reveals novel biomarkers. *Anal Bioanal Chem*. 2015;407:5065–77.
44. Liu R, Peng Y, Li X, Wang Y, Pan E, Guo W, et al. Identification of plasma metabolomic profiling for diagnosis of esophageal squamous-cell carcinoma using an UPLC/TOF/MS platform. *Int J Mol Sci*. 2013;14:8899–911.
45. Huang C, Freter C. Lipid metabolism, apoptosis and cancer therapy. *Int J Mol Sci*. 2015;16:924–49.